

# Constraints on Cosmic Neutrino Fluxes from the ANITA Experiment

S. W. Barwick,<sup>1</sup> J. J. Beatty,<sup>2</sup> D. Z. Besson,<sup>3</sup> W. R. Binns,<sup>4</sup> B. Cai,<sup>5</sup> J. M. Clem,<sup>6</sup> A. Connolly,<sup>7</sup> D. F. Cowen,<sup>8</sup> P. F. Dowkontt,<sup>4</sup> M. A. DuVernois,<sup>5</sup> P. A. Evenson,<sup>6</sup> D. Goldstein,<sup>1</sup> P. W. Gorham,<sup>9</sup> C. L. Hebert,<sup>9</sup> M. H. Israel,<sup>4</sup> J. G. Learned,<sup>9</sup> K. M. Liewer,<sup>10</sup> J. T. Link,<sup>9</sup> S. Matsuno,<sup>9</sup> P. Miočinović,<sup>9</sup> J. Nam,<sup>1</sup> C. J. Naudet,<sup>10</sup> R. Nichol,<sup>2</sup> K. Palladino,<sup>2</sup> M. Rosen,<sup>9</sup> D. Saltzberg,<sup>7</sup> D. Seckel,<sup>6</sup> A. Silvestri,<sup>1</sup> B. T. Stokes,<sup>9</sup> G. S. Varner,<sup>9</sup> and F. Wu<sup>1</sup>

<sup>1</sup>*Department of Physics and Astronomy, University of California at Irvine, Irvine, California*

<sup>2</sup>*Department of Physics, Ohio State University, Columbus, Ohio*

<sup>3</sup>*Department of Physics and Astronomy, University of Kansas, Lawrence, Kansas*

<sup>4</sup>*Department of Physics, Washington University in St. Louis, St. Louis, Missouri*

<sup>5</sup>*School of Physics and Astronomy, University of Minnesota, Minneapolis, Minnesota*

<sup>6</sup>*Bartol Research Institute, University of Delaware, Newark, Delaware*

<sup>7</sup>*Department of Physics and Astronomy, University of California at Los Angeles, Los Angeles, California*

<sup>8</sup>*Department of Astronomy and Astrophysics, Pennsylvania State University, University Park, Pennsylvania*

<sup>9</sup>*Department of Physics and Astronomy, University of Hawaii at Manoa, Honolulu, Hawaii*

<sup>10</sup>*Jet Propulsion Laboratory, Pasadena, California*

We report new limits on cosmic neutrino fluxes from the test flight of the Antarctic Impulsive Transient Antenna (ANITA) experiment, which completed an 18.4 day flight of a prototype long-duration balloon payload, called *ANITA-lite*, in early 2004. We search for impulsive events that could be associated with ultra-high energy neutrino interactions in the ice, and derive limits that constrain several models for ultra-high energy neutrino fluxes and rule out the long-standing Z-burst model. We set a 90% CL integral flux limit on a pure  $E^{-2}$  spectrum for the energy range  $10^{18.5} \text{ eV} \leq E_\nu \leq 10^{23.5} \text{ eV}$  at  $E_\nu^2 F \leq 1.6 \times 10^{-6} \text{ GeV cm}^{-2} \text{ s}^{-1} \text{ sr}^{-1}$ .

Cosmic rays of energy above  $3 \times 10^{19} \text{ eV}$  are almost certain to be of extragalactic origin. Their gyroradius far exceeds that required for magnetic confinement in our galaxy. At this energy pion photo-production losses on the cosmic microwave background radiation (CMBR) via the Greisen-Zatsepin-Kuzmin (GZK [1]) process limit their propagation distances to the local supercluster, of order 40 Mpc or less. However, the neutrinos that result from this process [2] would be observable out to the edge of the visible universe. Recent studies make compelling arguments that input from neutrino observations will be necessary to resolve the ultra-high energy cosmic ray (UHECR) problem [3]. Neutrinos are coupled to the highest energy cosmic rays both as a direct byproduct, and perhaps as a potential source of them. Straightforward reasoning indicates there is a required cosmogenic neutrino flux [2] with a broad peak in the energy range of  $10^{17-19} \text{ eV}$ . First, Lorentz invariance allows transformation of the cross section for photo-pion production at center-of-mass energies of order 1 GeV, the  $\Delta^+$ -resonance energy, up to GZK energies, a boost of order  $10^{11}$ . Second, precision measurements of the CMBR establish its flux density for all cosmic epochs and thus determine the number density of boosted targets for the photo-pion production process. Third, we apply the standard cosmological postulate that the cosmic-ray sources are not uniquely overdense (and hidden) in our local supercluster compared to the cosmic distribution. Finally, evidence from composition studies indicates that the UHECRs are hadronic, and thus unable to evade interaction with the CMBR, even if they are as heavy as iron [5]. We conclude that any localized source of UHECR at any epoch is surrounded by a “GZK horizon” beyond which the opacity of the CMBR to photo-pion interactions is sufficient to completely attenuate the charged progenitors, yielding pion secondaries which decay to neutrinos.

The intensity of all of these GZK neutrino spheres sums to a quasi-isotropic cosmogenic neutrino flux, unless any of the assumptions above is strongly violated, which would in turn constitute a serious departure from Standard Model physics.

Neutrinos may not only be cosmogenic byproducts, but could also be closely associated with sources of the UHECR, though this possibility is far more speculative. If there are large fluxes of neutrinos at energies of order  $10^{22-23} \text{ eV}$ , they can annihilate with Big-Bang relic cosmic background neutrinos ( $T_\nu \sim 1.9\text{K}$ ) in our own Galactic halo via the interaction  $\bar{\nu} \rightarrow Z^0$ , the *Z-burst* process [10, 11, 12, 13]. Decays of the neutral weak vector boson  $Z^0$  then yield UHECRs, overcoming the GZK cutoff because of the nearby production. Moreover, Topological Defect (TD) models [9] postulate a flux of super-heavy ( $10^{24} \text{ eV}$ ) relic particles that decay in our current epoch and within the Earth’s GZK sphere, yielding both neutrinos and UHECR hadrons in the process. Variant versions of such models, including hypothetical mirror-matter [14], can evade standard bounds to TD models; such variants currently have the weakest experimental constraints. Limits of the fluxes of ultra-high energy (UHE) neutrinos can constrain or eliminate such models as sources for the UHECR. Both of these classes of neutrino models predict fluxes well above the current predictions for cosmogenic GZK neutrinos. In all models, the neutrino fluxes in the  $10^{18-20} \text{ eV}$  energy range are well below what can be observed with a cubic kilometer target volume, so detection methods must use larger scales.

The ANITA mission is now completing construction for a first launch as a long duration balloon payload in 2006. The mission has a primary design goal of detecting EeV cosmogenic neutrinos, or providing a compelling flux limit. ANITA will detect neutrino interactions through coherent radio Cherenkov emission from neutrino-induced electromag-

netic (EM) particle cascades within the ice sheet. The ANITA-lite prototype flew as a piggyback instrument aboard the Trans-Iron Galactic Element Recorder (TIGER) payload. The payload launched Dec. 18, 2003, and was aloft for 18.4 days, spending a net 10 days over the ice in its 1.3 circuits of Antarctica. The payload landed on the ice sheet several hundred km from Mawson Station (Australia) at an elevation of 2500 m. ANITA-lite investigated possible backgrounds to neutrino detection in Antarctica and verified many of the subsystems to be used by the full-scale ANITA. The payload operation was successful, and we have searched for neutrino-induced cascades among the impulsive events measured. While ANITA-lite did not have adequate directional resolution to establish with certainty that the origin of any event was within the ice, the data quality was sufficient to distinguish events that were consistent with cascades, and exclude events which were not, thus enabling us to establish flux limits in the absence of candidate events.

ANITA exploits a property of EM cascades that has become known as the Askaryan effect [6]. During the development of the EM cascade, selective electron scattering processes lead to a negative charge asymmetry, inducing strong coherent radio Cherenkov radiation in the form of impulses with unique broadband spectral and polarization properties. When a high energy neutrino showers in the ice sheet, which has a radio attenuation length  $L_\alpha \geq 1$  km [15], the resulting impulses can easily propagate up through the surface to the balloon payload. From balloon altitudes of 37 km, the horizon is at nearly 700 km distance, giving a synoptic view of  $\sim 1.5$  M km<sup>2</sup> of ice, or  $\sim 2$  M km<sup>3</sup> volume to a depth of  $\simeq L_\alpha$ . ANITA will consist of a  $2\pi$  array of dual-polarization antennas designed to monitor this entire ice target. ANITA-lite flew only two first-generation ANITA antennas, with a field-of-view covering about 12% of the 1.5 M km<sup>2</sup> ice sheet area within its horizon at any time, but the  $\approx 170,000$  km<sup>2</sup> area of ice in view still represents an enormous monitored volume for the uppermost kilometer of ice to which we were primarily sensitive. This leads to the strongest current limit on neutrino fluxes within its energy regime.

The ANITA-lite antennas are dual-linear-polarization vertical (V) and horizontal (H) quad-ridged horn antennas, sensitive over 230-1200 MHz, over which their angular response remains single-mode, with a nearly constant effective directivity-gain of about 9-11 dBi. The antenna beam is somewhat ellipsoidal in shape, with average beamwidths of 59° and 37° in E-plane and H-plane, respectively. The antenna boresights were offset from one another by 1 m lateral separation, 22.5° in azimuth, and were canted 10° downward in elevation. The antennas were designed to retain an off-axis directivity of  $\geq 6$  dBi at the angles corresponding to the boresights of the adjacent antennas; thus each antenna retains good sensitivity to trigger on events that are centered on its nearest neighbor's field-of-view. The combined field-of-view of the two antennas taken in coincidence is of order 45° in azimuth for typical events, but can be significantly larger for strong impulses.

A block-diagram of the ANITA-lite antenna, trigger, and

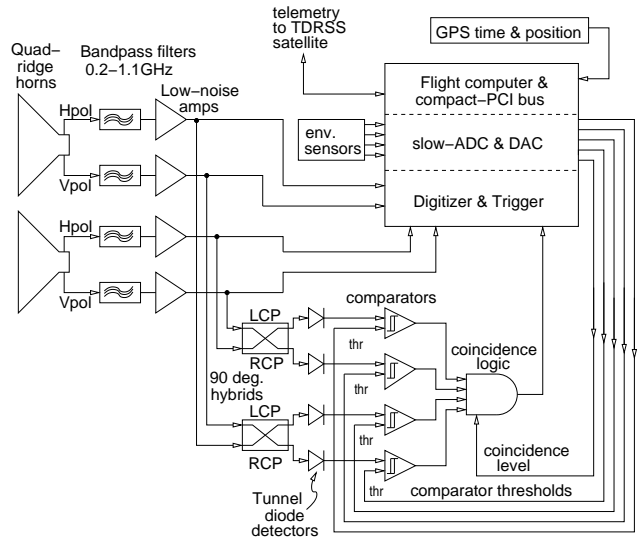


FIG. 1: The ANITA-lite system block diagram.

data acquisition system is shown in Fig. 1. The H- and V-polarization antenna voltages are first filtered to limit the pass-band to 0.2–1.1 GHz. A notch filter (not shown) removes a region around 400 MHz used by payload telemetry. The signals are amplified by low-noise amplifiers (LNAs) with approximately 100 K noise figure, for a net gain of  $\sim 62$  dB. The resulting signals, with thermal-noise levels corresponding to  $\sim 35$  mV rms, are split equally between the digitizers and the trigger coincidence section.

Coherent Cherenkov emission from showers in solid media is 100% linearly polarized [7], and Antarctic ice does not produce significant depolarization over the propagation distances ( $\sim 1$  km) required for detection of neutrino interactions [16]. ANITA-lite takes advantage of this characteristic by requiring that any trigger have roughly equal amplitude in left- and right-circular polarizations (LCP & RCP). This favors signals with a high degree of linear polarization, and provides of order a factor of two improvement in rejecting circularly-polarized backgrounds. The conversion from the H- and V-polarizations received from the antenna into LCP and RCP is done by broadband 90° hybrid-mode combiners.

The trigger system is critical to the sensitivity of a radio impulse detection system. It initiates digitization of antenna waveforms based on correlated pulse amplitudes among the different antenna channels. For ANITA-lite, the trigger required a 1- to 3-fold coincidence among the four independent channels (two antennas and two polarizations), where each channel was required to exceed a power threshold during a 30 ns window. The pulse-height spectrum of received voltages due to ideal thermal noise is nearly Gaussian, and ANITA-lite was operated with an average threshold corresponding to  $4.3 \sigma_V$ , where  $\sigma_V = \sqrt{k \langle T_{sys} \rangle Z \Delta \nu}$  for bandpass-averaged system temperature values of  $\langle T_{sys} \rangle \approx 700$  K during the flight. Here  $k$  is Boltzmann's constant,  $Z = 50 \Omega$ , and  $\Delta \nu = 800$  MHz

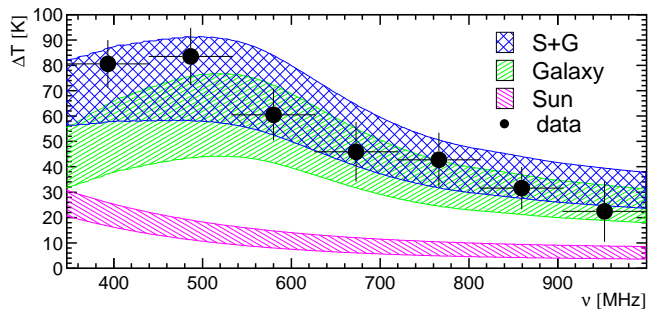


FIG. 2: (Color online) Frequency dependence of the excess effective antenna temperature  $\Delta T$  when pointing to the Sun and the Galactic Center [32]. The top band is a model of the expected  $\Delta T$ , with a width equal to the systematic uncertainties. The lower two bands give contributions due to galactic and solar emissions, respectively. The antenna frequency response is folded into the model.

is the system bandwidth.

Calibration of the system gain, timing, and noise temperature was performed by several means. A calibrated noise diode was coupled to the system between the antenna and the first bandpass filter. Also, during the first day of the flight, a pulse generator and transmitter antenna at the launch site (Williams field, near McMurdo Station) illuminated the payload with pulses synchronized to GPS signals. An onboard GPS signal synchronously triggered the ANITA-lite system. These pulses were recorded successfully by the system out to several hundred km distance. Timing analysis of these signals indicates that pulse phase could be estimated to a precision of 150 ps for  $\geq 4\sigma$  signal-to-noise ratio. Finally, the response of the antennas to broadband noise from both the Sun and the Galactic center and plane was determined by differential measurements using data when the payload (which rotated slowly during the flight) was toward or away from a given source. The results of this analysis are shown in Fig. 2, showing the spectral response function with the various contributions from astronomical sources. The ambient RF noise levels at balloon float altitudes were found to be consistent with thermal noise due to the ice at  $T_{eff} \sim 250$  K and our receiver noise temperature of 300 – 500 K, which included contributions from the cables, LNA, connectors, filters, and power limiters. Other than our own ground calibration signals, we also detected no sources of impulsive noise that could be established to be external to our own payload. Several types of triggers were investigated for correlations to known Antarctic stations, and no such correlations were found.

ANITA-lite recorded  $\sim 113,000$  events at an average live-time of 40% [23]. Of these events,  $\sim 87,500$  are 3-fold-coincident triggers considered for data analysis. The remainder were recorded for system calibration and performance verification. Two independent analyses were performed within collaboration, both searching for narrow Askaryan-like impulses, in which almost all signal power is delivered within 10 ns about peak voltage, time-coincident in at least two of four channels. Analysis A primarily relied on matched-

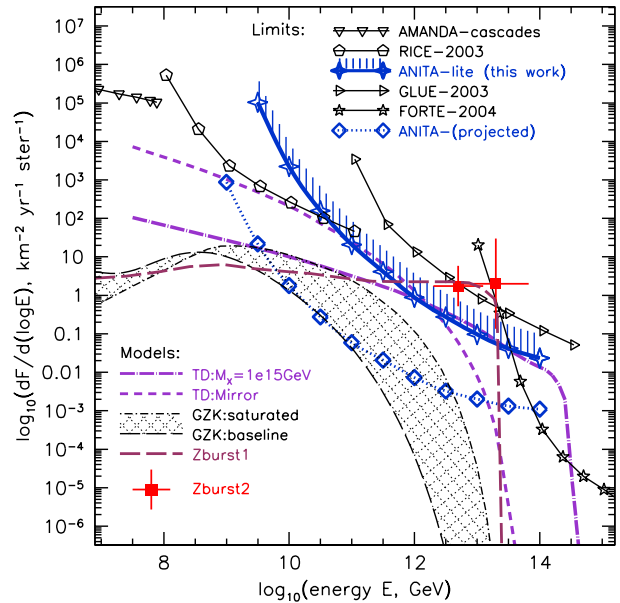


FIG. 3: (Color online) Limits on various models for neutrino fluxes at EeV to ZeV energies. The limits are: AMANDA cascades [27], RICE [29], the current work, GLUE [30], the FORTE satellite [31], and projected sensitivity for the full ANITA. Models shown are Topological Defects for two values of the X-particle mass [9], a TD model involving mirror matter [14], a range of models for GZK cosmogenic neutrinos [4, 21, 22], and several models for Z-bursts [11, 20]. In the Z-burst models plotted as points, the flux is a narrow spectral feature in energy, and the error-bars shown indicate the range possible for the central energy and peak flux values.

filtering the data with the expected signal shape and requiring the filtered data to show better signal-to-noise ratio than the unfiltered data. Analysis B primarily relied on rejecting events which show high level of cross-correlation with known payload-induced noise events. This approach very efficiently removes the very common repetitive payload noise events. These constituted about 90% of triggers, with the remainder from unknown sources, probably also on the payload. None of these resembled the expected neutrino signals. Analysis A determined the signal passing efficiency by tightening the cuts until the last background noise event was removed, and found 53% of the simulated signal still passing the cuts. Analysis B blinded 80% of the data, optimized the cuts with the other 20% using the model rejection factor technique [24], and found 65% signal efficiency. No data events pass either of the analyses. In both analyses, the systematic uncertainty in passing rates was estimated at  $\sim 20\%$ .

To estimate the effective neutrino aperture and exposure for ANITA-lite, two different and relatively mature simulation codes for the full ANITA instrument were modified to account for the ANITA-lite configuration. These simulations account for propagation of neutrinos through earth crust models, for the various interaction types and neutrino flavors, for inelasticity, and both hadronic and electromagnetic interactions (including LPM effects [25]). The shower radio emis-

sion is estimated via standard parameterizations which have been validated at accelerators [7, 26]. Propagation through the ice uses a frequency- and temperature-dependent model for  $L_\alpha$ , based on data measured at the South Pole [15]. Surface refraction is accounted for using a combination of ray- and physical-optics. Refracted emission is propagated geometrically to the payload where a detailed instrument model, based on lab measurements of the spare flight system, is applied to determine whether a detection occurs.

Based on the treatment described in Refs. [28, 31], the resulting model-independent 90% CL limit on neutrino fluxes with Standard Model cross-sections [18] is shown in Fig. 3. ANITA-lite approaches the highest energy cosmogenic neutrino flux model [22], and now appears to have entirely excluded the Z-burst model [8, 11, 13] at a level required to account for the fluxes of the highest energy cosmic rays, as represented by the two crosses in the figure, with vertical and horizontal bars indicating the range of allowed model parameters for this case. Prior limits from the GLUE and FORTE experiments had constrained most but not all of this range. Our limits rule out all of the remaining range for two of the highest standard topological defect models, shown in Fig. 3, both of which were constrained already by other experiments. We also provide the first experimental limits on the highest mirror-matter TD model [14]. Table I shows the expected event totals and limits for several of these models. The ANITA-lite 90% CL integral flux limit on a pure  $E^{-2}$  spectrum for the energy range  $10^{18.5} \text{ eV} \leq E_\nu \leq 10^{23.5} \text{ eV}$  is  $E_\nu^2 F \leq 1.6 \times 10^{-6} \text{ GeV cm}^{-2} \text{ s}^{-1} \text{ sr}^{-1}$ .

TABLE I: Expected numbers of events from few UHE neutrino models, and confidence level of exclusion by ANITA-lite observations.

Model & references	Events	CL,%
Baseline GZK models [4, 21, 22]	0.009	...
Strong source evolution GZK models [4, 20, 22]	0.025-0.048	...
GZK Models that saturate all bounds [20, 22]:	0.48 to 0.60	38 to 45
<i>Topological Defects:</i>		
Yoshida <i>et al.</i> 1997, $M_X = 10^{16} \text{ GeV}$ [9]	7.8	99.959
Yoshida <i>et al.</i> 1997, $M_X = 10^{15} \text{ GeV}$ [9]	22	100.000
Berezinsky 2005, Mirror Necklaces [14]	6.4	99.834
<i>Z-burst Models:</i>		
Fodor <i>et al.</i> (2002): Halo background [11]	5.0	99.326
Fodor <i>et al.</i> (2002): Extragalactic background [11]	14.2	99.999
Kalashhev <i>et al.</i> (2002) [10]	45.9	100.000

Although designed primarily as an engineering test, ANITA-lite has set the best current limits on neutrino fluxes above  $10^{19.5} \text{ eV}$ , improving constraints by more than an order of magnitude over the GLUE results [30]. This demonstrates the power of the radio Cherenkov technique applied to

the balloon-based observations of the Antarctic ice. Simulations for ANITA shown in Fig. 3, indicate totals of order 5-50 events for the GZK model range shown for 50 days of flight time, sufficient to detect these model fluxes for the first time.

This work has been supported by NASA. We thank the Columbia Scientific Balloon Facility and the National Science Foundation for their excellent support of the Antarctic campaign.

- 
- [1] K. Greisen, Phys. Rev. Lett. **16** (1966) 748; G. T. Zatsepin and V. A. Kuz'min, JETP Letters **4** (1966) 78.  
[2] V. S. Berezinsky and G. T. Zatsepin, Phys. Lett. **28B** (1969) 423; Sov. J. Nucl. Phys. **11** (1970) 111; F. W. Stecker, Astrophys. Space Sci. **20** (1973) 47; Ap. J. **238** (1979) 919.  
[3] D. Seckel and T. Stanev, Phys. Rev. Lett. **95** (2005) 141101.  
[4] R. Engel, D. Seckel, and T. Stanev, Phys. Rev. **D64** (2001) 093010.  
[5] R. Abbasi *et al.*, Astrophys. J. **622** (2005) 910  
[6] G. A. Askaryan, JETP **14** (1962) 441; JETP **21** (1965) 658.  
[7] D. Saltzberg *et al.*, Phys. Rev. Lett. **86** (2001) 2802; P. W. Gorham *et al.*, Phys. Rev. **E62** (2000) 8590.  
[8] B. Eberle *et al.*, Phys. Rev. **D70** (2004) 023007  
[9] S. Yoshida *et al.*, Ap. J. **479** (1997) 547.  
[10] O. E. Kalashev *et al.*, Phys. Rev. **D65** (2002) 103003.  
[11] Z. Fodor, S. D. Katz, and A. Ringwald, Phys. Rev. Lett. **88** (2002) 171101.  
[12] T. J. Weiler, Astropart. Phys. **11** (1999) 303.  
[13] T. Weiler, Phys. Rev. Lett. **49** (1982) 234.  
[14] V. Berezinsky, Proc. of 11<sup>th</sup> Int. Workshop Neutrino Telescopes (ed. Milla Baldo Ceolin, 2005) p. 339; astro-ph/0509675.  
[15] S. Barwick *et al.*, J. Glaciol. **51** (2005) 231.  
[16] N. D. Hargreaves, J. Glaciol. **21** (1978), 301; C. S. M. Doake, Geophys. J. Roy. Astr. S. **64** (1981) 539.  
[17] T. Furukawa, K. Kamiyama and H. Maeno, Proc. NIPR Symposium on Polar Meteorology and Glaciol. **10** (1996) 13.  
[18] R. Gandhi, Nucl. Phys. Proc. Suppl. **91** (2000) 453.  
[19] E. Zas, F. Halzen, and T. Stanev, Phys. Rev. **D45** (1992) 362.  
[20] O. E. Kalashev, *et al.*, Phys. Rev. **D66**, 063004 (2002).  
[21] R. J. Protheroe & P. A. Johnson, Astropart. Phys. **4** (1996) 253.  
[22] C. Aramo *et al.*, Astropart. Phys. **23** (2005) 65.  
[23] This relatively low livetime was caused by a software bug leading to a slow readout of the GPS time for each event.  
[24] G. C. Hill and K. Rawlins, Astropart. Phys. **19** (2003) 393.  
[25] J. Alvarez-Muñiz and E. Zas, Phys. Lett. **B411** (1997) 218.  
[26] P. Gorham *et al.*, Phys. Rev. **D72** (2005) 023002.  
[27] M. Ackermann *et al.*, Astropart. Phys. **22** (2004) 127.  
[28] L. A. Anchordoqui *et al.*, Phys. Rev. **D66** (2002) 103002.  
[29] I. Kravchenko *et al.*, Astropart. Phys. **20** (2003) 195.  
[30] P. W. Gorham *et al.*, Phys. Rev. Lett. **93** (2004) 041101.  
[31] N. Lehtinen, P. W. Gorham, A. R. Jacobsen, and R. A. Roussel-Dupré, Phys. Rev. **D69** (2004) 013008.  
[32] The band from 230-350 MHz had higher  $T_{\text{sys}}$  and is excluded here due to the low precision of the measurement.